# Dynamics of circulation control using surface plasma actuators for aerodynamic load alleviation on wind turbine airfoils

Annie Leroy, Pierrick Joseph, Sophie Baleriola, Dominique Nelson-Gruel, Sandrine Aubrun, Yahia Haidous, Stéphane Loyer, Philippe Devinant

# Circulation control using surface plasma actuators for aerodynamic load alleviation on wind turbine airfoils

**P. JOSEPH, A. LEROY, S. BALERIOLA, D. NELSON-GRUEL, Y. HAIDOUS, S. LOYER, P. DEVINANT, S. AUBRUN**

Université d'Orléans, INSA CVL, PRISME, EA 4229, F-45072, Orléans, France
annie.leroy@univ-orleans.fr

## Abstract:

*Due to changing atmospheric conditions, the incoming wind reaching a wind turbine is highly unsteady and inhomogeneous and therefore entrains gusts that may induce significant fatigue loads on the wind turbines. By reducing these load fluctuations, the lifespan of the wind turbine rotors could be extended and the energy production optimized. In this context, the objectives of the present experimental work is to demonstrate the possibility to maintain a constant lift force for a wind turbine airfoil in response to gusts modifying its angle of attack by using active flow control (AFC) techniques. Then, the present study aims at investigating experimentally the potentialities of surface plasma actuators to achieve circulation control and to perform model identification in view of developing a closed loop control approach.*

**Keywords:** circulation control, surface plasma actuator, wind turbine airfoil, system identification.

## 1 Introduction

Due to inhomogeneous and unsteady incoming wind conditions, it is expected that wind turbine airfoils under real operating conditions may encounter angle of attack variations of around ±5° inducing load fluctuations to mitigate. It is then necessary to optimize the wind energy efficiency and the rotor lifespan by developing innovative control concepts with the intention of reducing load fluctuations on blades.

Strategies of circulation control acting at the blade airfoil trailing edge are usually investigated to allow lift increase and decrease. The displacement of the streamline separation point and of the rear stagnation point is allowed on a rounded trailing-edge airfoil. This flow modification at the trailing-edge permits the monitoring of the circulation and consequently a regulation of the lift force that can be either increased or decreased. For aerodynamic bodies, they are traditionally implemented by means of concepts including shape change, flaps, blowing, suction, etc., and often make use of the Coanda effect that keeps a tangential jet attached over a curved surface [1-3].

This paper focuses on the presentation of results obtained and analyzed in view of developing a close loop control approach. Fig. 1 shows the principle of this circulation control actuation in response to a gust modifying the angle of attack. The aim of this flow control is to maintain a constant lift force

whatever the incoming wind conditions are. The working range of angles of attack is located along the linear part of the lift curve where the flow is attached to the airfoil.

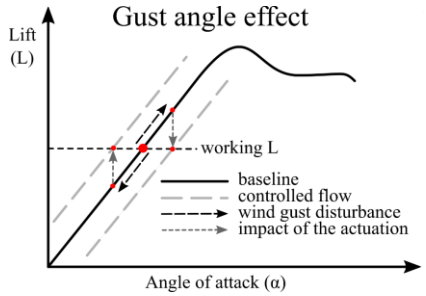


Figure 1. Principle of circulation control in response to a sudden gust modifying the angle of attack.

Firstly, the potentialities of such a circulation control technique by using plasma actuators is validated by conducting experimental testing. Interest in plasma actuators (PA) for flow control has been largely reported in the literature over the last decade. Recent studies have dealt with control circulation by surface (PA) [4-5] in which the feasibility of this strategy was demonstrated. Even though PA are characterized by quite low momentum coefficients, one of their main advantageous features for control applications is their short time response lower than the millisecond.
Surface pressure, load and velocity field measurements in the large subsonic wind tunnel of PRISME laboratory were performed to evaluate the actuator effectiveness and to highlight the flow mechanisms induced by the actuation for lift increase and decrease configurations. Secondly, system identification theory was used to build a model of the system, in order to be used in a closed-loop control. The chosen input variable was the high voltage amplitude and the chosen output variables were the surface pressure levels obtained with 20 pressure taps distributed along the chord that permit to characterize the lift force increase variation. Results permitted to extract involved time scales and to identify the system for some operating points. Interestingly, the system was found to behave like a piecewise linear systems when using wisely chosen pressure taps. This model allows then to correctly predict the lift force in controlled cases.

# 2 Experimental set up

## 2.1 Facilities and measurement

The experiments were carried out in the closed return wind tunnel of the PRISME laboratory at the University of Orleans. An airfoil having a NACA$65_4$-421 profile section with a rounded trailing edge has been specifically designed for PA implementation purposes as shown in Fig. 2. More details on the aerodynamic performances are described in [6]. The model has a chord of $c$ = 300mm and a wing span of 1.1m. The airfoil was mounted horizontally between two vertical flat plates in order to achieve a 2D flow configuration into the 5m long main test section with a cross-section of 2m × 2m. It was mounted on both tips onto a platform balance used for time-averaged lift and drag measurements and located under the test section. The balance was carefully calibrated, lift and drag coefficient uncertainties were estimated to be less than 5% for the lift force and 10% for the drag force for the reference velocity considered in the present experiments. In this study, the operating speed of the wind tunnel is 10m/s with an airflow turbulence level below 0.4%. It leads to a chord-based Reynolds number of $Re = 2 \times 10^5$.

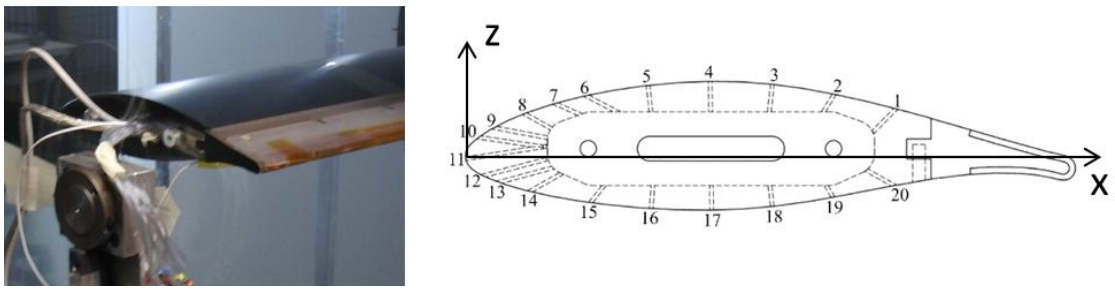


Figure 2. Photography of the airfoil model mounted on the wind tunnel test section (left) and position of the pressure taps (right).

Mean pressure distribution around the airfoil was measured with pressure taps implemented around the model. 20 pressure taps are available in the median section. It was not possible to implement pressure taps along the trailing edge part dedicated to support the actuator. Mean velocity fields around the airfoil trailing edge were studied from 2D-PIV measurements in order to analyze flow topology in streamwise planes of the airfoil model and more particularly in the median plane ($y$ = 0mm). The PIV system consisted, in the case of the wind-tunnel experiments, in a Nd:YAG laser (2 × 200mJ) emitting pulses with a 2.5Hz emission rate. The light sheet was oriented in order to visualize simultaneously both pressure and suction sides of the airfoil. Seeding particles were micro-sized olive oil droplets sprayed by a PIVTEC seeding system. Images were acquired with a LaVision Imager LX camera (4032px × 2688px) and a 200mm lens. 1,000 image pairs were recorded. Images processing was carried out with DaVis 8.3 LaVision software and the final resolution is of one vector every 0.4mm with a 32px × 32px interrogation window with an overlap of 50%. For the quiescent air experiments, the same seeding system was used as well as a similar laser. The camera used was a TSI Power View (2048px × 2048px) with a 200 mm lens. 600 image pairs were recorded for every configuration. This system allows a final resolution of one vector every 0.5mm with a 32px × 32px interrogation window.

## 2.2 Description of DBD actuators

Plasma actuators consisted in an arrangement of two successive Dielectric Barrier Discharges (DBD). As it can be assumed that the flow induced by the actuator behaves like a two-dimensional wall jet, it allows to perform a bi-dimensional action on the flow. Fig. 3 shows the section view of the trailing edge airfoil section equipped with the PA made of two successive single DBD. One single DBD consists in two copper electrodes that are positioned on both sides of a dielectric material (PMMA, 3 mm thick) of the model cap. The high voltage electrodes (or active electrodes) are serrated and powered with an AC-power supply up to 18kV and at 1kHz, while the grounded one is linear and encapsulated within the dielectric material of the model itself. The high voltage and grounded electrodes were 950mm long, while the length of the floating electrode was 900mm. With a high voltage application at the active electrode, the ambient air is ionized and accelerated, creating an ionic wind along the grounded electrode that permits the manipulation of the flow near the wall area. Plasma is generated from the first high voltage electrode. For such an actuator, the electrical power consumption was measured and estimated at around 80 W/m. It was characterized in quiescent air conditions by PIV in the median airfoil section. As shown in Fig. 4, the ambient air is deflected towards the plasma region with an acceleration close to the wall, highlighting the higher velocity at the plasma-gas interface along the whole actuator. Downstream of the main actuation zone, one can observe diffusion of the induced jet on the normal direction to the wall. The velocity vector profiles suggest that the wall jet expands away from the wall because of the curvature resulting in a widened jet in the pressure side zone with slight lower streamwise velocities.

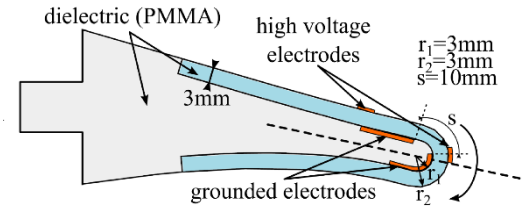


Figure 3. Scheme of the trailing edge equipped with the DBD actuator named ACT1.

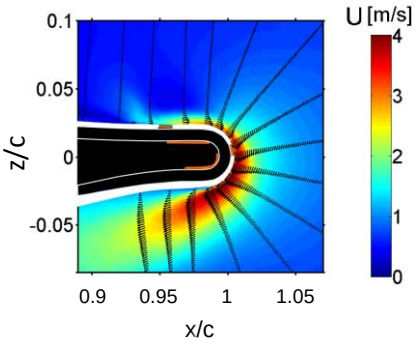


Figure 4. Time averaged magnitude velocity contours and velocity vector profiles of the flow induced by the DBD actuator in quiescent air (18kV, 1kHz).

The momentum coefficient $C_\mu$, the typical figure of merit for discussing the circulation control efficiency, has been estimated. It was chosen to estimate the momentum coefficient by integration of the tangential velocity profile in the wall normal direction, in the plasma region, just at the downstream edge of the second grounded electrode, as done in [4] or [7].

(1) $$C_\mu = \frac{\int_0^\infty \rho u^2(z)\, dz}{\frac{1}{2}\rho_\infty U_\infty^2 c}$$

Based on these results, for a freestream flow of $U_\infty$ = 10 m/s, within this work, $C_\mu$ was about 0.004.

# 3 Open-loop control of lift system

Firstly, an open-loop control approach using PA was performed to assess the potentialities of a type of circulation control. Surface pressure, aerodynamic load and velocity field measurements were performed to evaluate the actuator effectiveness and to highlight the flow mechanisms induced by the actuation for lift increase configurations.

Fig. 5 shows the lift coefficient at different angles of attacks (AOA, denoted by $\alpha$) in baseline conditions and with ACT1 in operation at $U_\infty$ = 10 m/s. The lift coefficient variation obtained depends on electrical operating parameters chosen for powering the plasma actuator. Considering the electric limitations due to plasma generation, the maximum lift coefficient variation obtained was $\Delta C_L = +0.08$. It can be observed that the increment in the lift is nearly the same for the different AOA investigated with actuation for which the flow is fully attached. Regarding the lift to drag ratio on Fig. 6, the curve is also modified under plasma actuation. The actuator increases the lift to drag ratio for AOA between $\alpha$ = -7° and $\alpha$ = +5° and for higher angles of attack the modified curve is superimposed to the baseline. It shows that the actuation effect did not engender penalty in drag. From these results it can be deduced that the effects of the plasma actuation resulted in an absolute variation of +1° in AOA.

Static pressure measurements are used to assess the modification of aerodynamic forces with actuation. In Fig. 7 the pressure distribution is plotted for AOA of $\alpha$ = 0° and $\alpha$ = 5° in baseline configuration and with actuation. Compared to the pressure distribution without actuation, the whole pressure distribution around the airfoil is modified under actuation. Pressure distribution is decreased on the suction side and slightly increased on the pressure side, resulting by integration along the side walls, in higher normal pressure force and lift force.

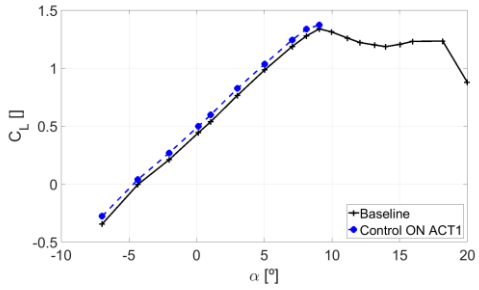


Figure 5. Lift coefficient versus angle of attack. Re = 2 × $10^5$ ; (18kV, 1kHz).

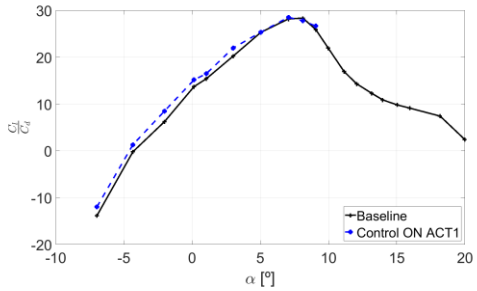


Figure 6. Lift to drag ratio versus angle of attack. Re = 2 × $10^5$ ; (18kV, 1kHz).

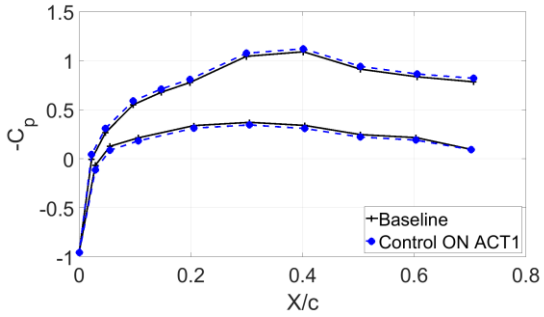


(a) α = 0°

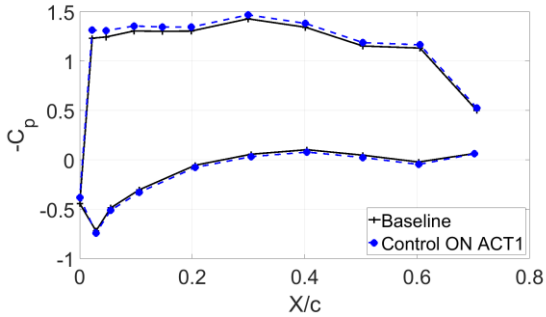


(b) α = 5°

Figure 7. Pressure distribution along the chord airfoil without and with actuation. Re = 2 × $10^5$ ; (18kV, 1kHz).

The actuation tends to deviate the wake towards the pressure side as shown in Fig. 8 where the longitudinal velocity profiles within the wake at 5% of the chord downstream the trailing-edge for $\alpha = 0°$ are extracted from mean velocity fields obtained by PIV.

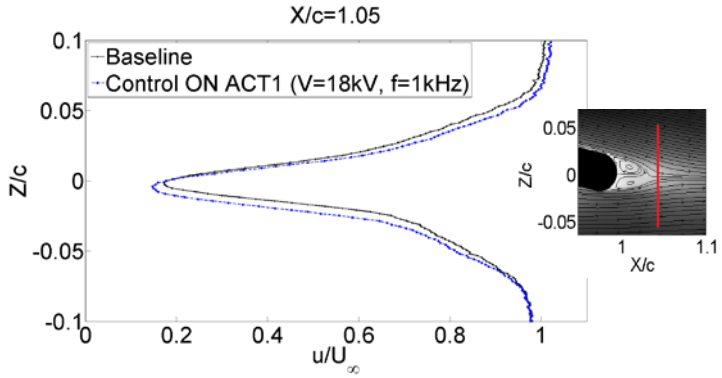


Figure 8. Longitudinal velocity profiles without and with actuation. α = 0°; Re = 2 × $10^5$ ; (18kV, 1kHz).

# 4 Model identification

Mitigation problem of load fluctuations encountered by the profile could be solved or investigated using a closed loop control of the lift coefficient ($C_L$) but lift sensor is rarely available on industrial systems (i.e. wind turbine). A real time dynamical lift model is proposed and validated through comparison with value of lift given by an aerodynamic balance placed on the current experimental setup. This sensor has a strong delay and could not be embedded on a wind turbine consequently it cannot be used to build a control loop. As a first step to build this virtual sensor, one proposes to get a better understanding of the system by identifying the associated simplified dynamic model. Main goals are to choose a quantity to be controlled, but also to identify the linear or non-linear behaviour of the system. These last results will provide relevant information to determine the type of control loop that could be implemented. This model will be also used to estimate the effect of the control action, and to detect any unwanted behaviour of the plasma actuation during the future closed loop experiments.

## 4.1 System definition

System is composed of the plasma actuator (including the low frequency generator used to generate the command signal), the airfoil profile and the sensors. In the present paper, one considers only the aerodynamic balance and the twenty pressure taps distributed in the model middle plane and linked to a pressure sensor (see Fig. 9). Consequently, system's input is $U_{GBF}$ (input voltage of the generator), and systems outputs consist in load and pressure measurements. As depicted on Fig. 9, calibration of the actuator reveals that a linear relation exists between input voltage of the generator and voltage imposed to the plasma actuator ($U_{plasma}$), so in the following, one can also considers $U_{plasma}$ as the input parameter.


Figure 9. System definition.

## 4.2 System excitation

The system is submitted to variations of the input parameter $U_{plasma}$ following several step patterns (an example is depicted on Fig. 10, left). Output signals are recorded for every sensors. Responses observed on the pressure sensor greatly differs depending on the considered pressure tap. Tap #5 is particularly interesting as, in the static case, its response is piecewise-linear to the input parameter variation (see Fig. 10, right). From a dynamic point of view, the piecewise-linear properties of the system lead to the possibility to identify the system by linear transfer function around some operating points (see Fig. 11).

Fig. 12 presents some results of lift measurements obtained with balance versus the pressure on the tap #5 for various angles of attack and several $U_{plasma}$ values. Considering linear steady state behaviours (Fig. 10 and 12) there is clearly a linear relationship between the lift coefficient and this particular pressure tap. The pressure tap #5 appears to be a convenient solution to build the control loop. It is important to stress that this is not the case with all pressure taps.

The existence of any dynamic effect between the lift and the pressure tap #5 is under investigation and will be addressed in a near future. Taking into account that only slow variations of angle of attack in comparison to the chord time scale are considered, one assumes that there is no dynamic effect in that case and that the dynamic part of the relationship between the lift and the pressure at this point can be approximated by a succession of static states.

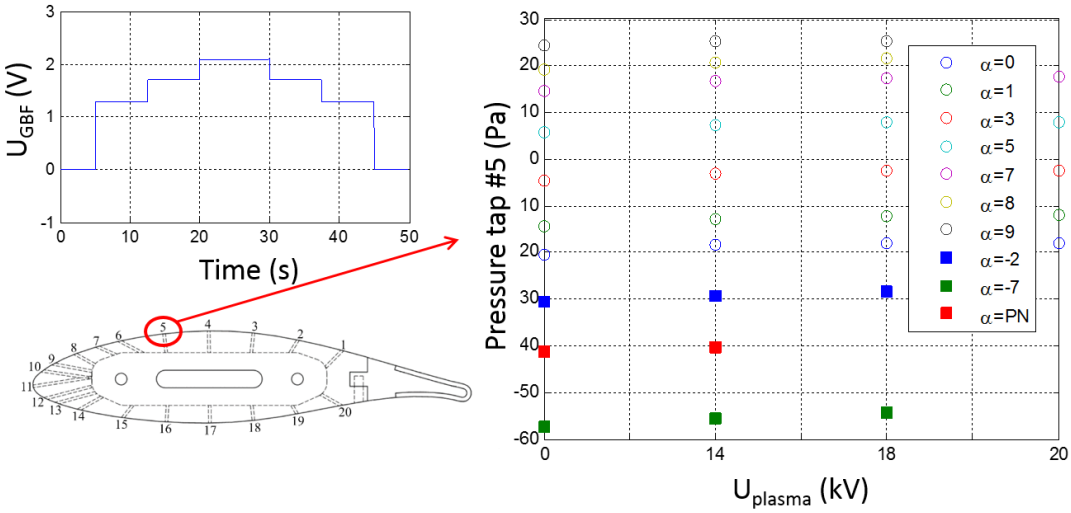


Figure 10. System excitation and static response.
α = PN corresponds to the angle of attack where lift is null.

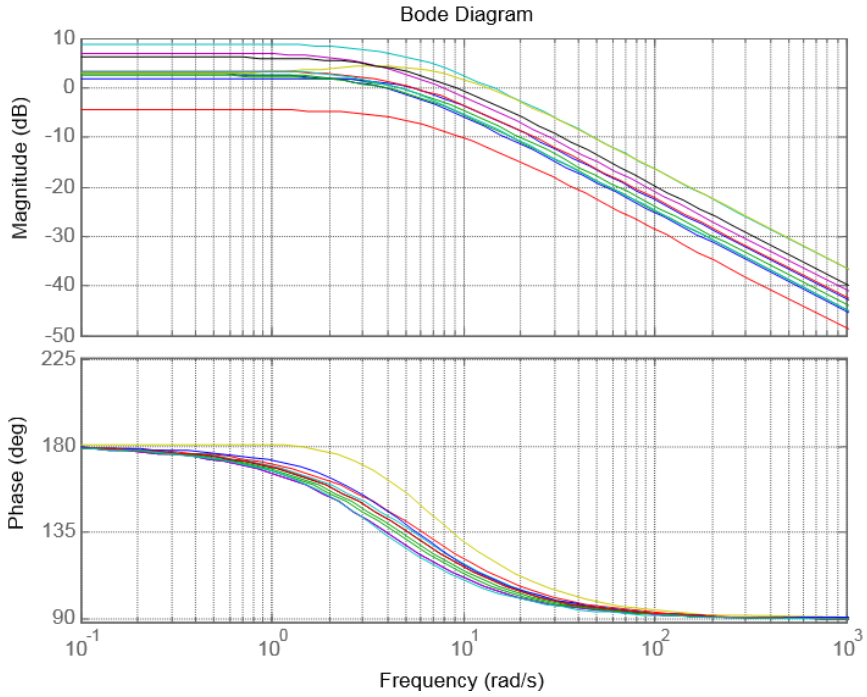


Figure 11. Linear transfer functions of the system identified around different operating points.

## 4.3 Model validation

Fig. 13 presents a first assessment of the dynamical model. The input signal and the experimental data depicted below come from another dataset and were not used to build the model. Despite the important

noise present on the experimental data, one observes a good agreement of the mean measured lift compared with the one computed by the model. This is only partially true with the pressure, as for time superior to 30s on the middle graph, one observes some differences between measurements and computed values. Next test campaign will be focused, among other things, on improving this model. The behaviour of the plasma actuator for low input voltage has to be checked in particular.

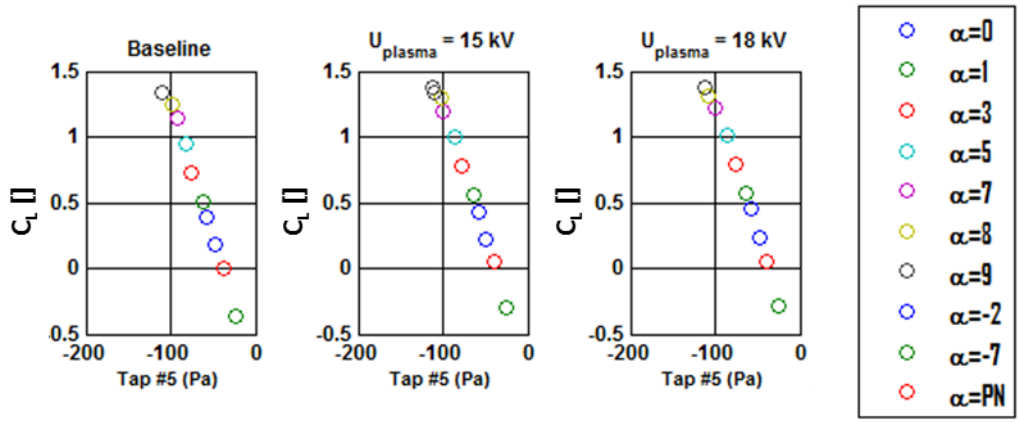


Figure 12. Lift coefficient function of the pressure on the tap #5 for various angles of attack: baseline (left), $U_{plasma}$ = 15kV (middle) and $U_{plasma}$ = 18kV (right). α = PN corresponds to the angle of attack where lift is null.

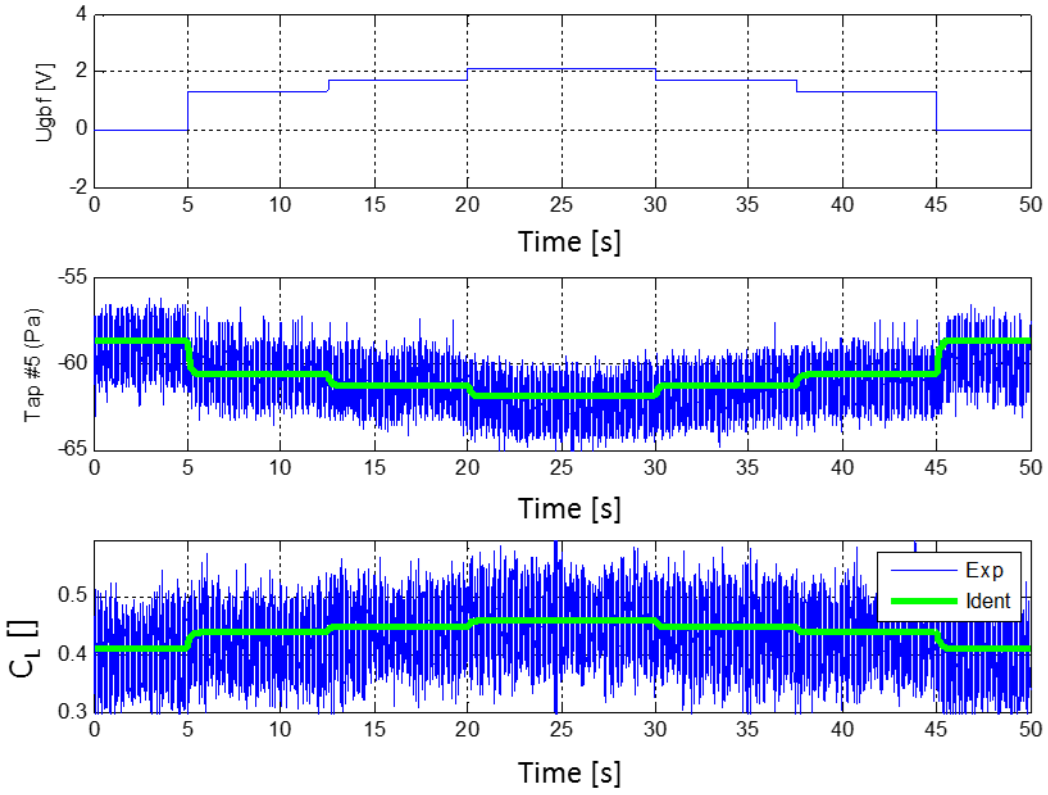


Figure 13. Comparison between experiment and mathematical model for the pressure recorded by pressure tap #5 (middle graph) and the lift coefficient (bottom graph). This dataset was not used to build the model.

# 5 Conclusion

The results presented in this experimental study have shown the possibility to increase the lift for a realistic modified 2D wind turbine blade ($NACA65_4$-421 profile) by applying surface plasma actuation at its rounded trailing edge. A lift increment up to around 0.1 could be obtained by plasma actuation corresponding to a variation of +1° in angle of attack. The final objective of the experimental work is to demonstrate in a wind tunnel scale the possibility to maintain a constant lift force for a wind turbine airfoil in response to gusts modifying its angle of attack. That will be achieved by developing a closed loop control approach. As a first step to build this closed loop, it has been proposed to get a better understanding of the system by identifying the associated mathematical model which relates static pressures and lift measured during the experiments. From a static point of view at the vicinity of the considered operating angle attack, a linear relationship between the lift coefficient and specific pressure taps has been detected. These results will provide first information to determine the kind of regulation to be used in the closed loop.

# Acknowledgments

This project is funded by the national French project SMARTEOLE (ANR-14-CE05-0034).

# References

[1] R. D. Joslin and G. S. Jones, Progress in astronautics and aeronautics 214 AIAA Inc. (2006).

[2] J. Kweder, C.C. Panther and J. E. Smith, (2010), Int. J. Eng (4), pp411–429.

[3] S. J. Johnson, C.P. Case van Dam and D. E. Berg, Active Load Control Techniques for Wind Turbines SANDIA Report, (2008).

[4] P. F. Zhang, B. Yan, A.B. Liu and J. J. Wang, (2010), AIAA Journal (48) 10.

[5] M. Kotsonis, R. Pul and L. Veldhuis, (2014), Exp. in Fluids (55):1772.

[6] S. Aubrun, A. Leroy, P. Devinant, (2015), Proc. in 50th 3AF International Conference on Applied Aerodynamics, Toulouse, France, March 29-30 – April 01.

[7] R. Sosa, G. Artana, E. Moreau and G. Touchard, (2007), Exp. in Fluids (42), pp143–167.